JoP Journal of Pharmacopuncture

Journal of Pharmacopuncture 2024;27(1):1-13
pISSN: 2093-6966 • eISSN: 2234-6856
https://doi.org/10.3831/KPI.2024.27.1.1

Original Article

Check for updates

Enhanced Drug Carriage Efficiency of Curcumin-Loaded PLGA Nanoparticles in Combating Diabetic Nephropathy via Mitigation of Renal Apoptosis

Asmita Samadder[1]*, Banani Bhattacharjee[1], Sudatta Dey[1], Arnob Chakrovorty[1], Rishita Dey[1,2], Priyanka Sow[1], Debojyoti Tarafdar[3], Maharaj Biswas[4], Sisir Nandi[2]

[1]Cytogenetics and Molecular Biology Laboratory, Department of Zoology, University of Kalyani, Kalyani, India
[2]Department of Pharmaceutical Chemistry, Global Institute of Pharmaceutical Education and Research, Veer Madho Singh Bhandari Uttarakhand Technical University, Kashipur, India
[3]Department of Chemistry, Chanchal College, Affiliated to The University of Gour Banga, West Bengal, India
[4]Endocrinology and Reproductive Biology Laboratory, Department of Zoology, University of Kalyani, Kalyani, India

Received June 16, 2023
Reviewed July 23, 2023
Accepted December 18, 2023

***Corresponding Author**
Dr. Asmita Samadder
Cytogenetics and Molecular Biology Laboratory, Department of Zoology, University of Kalyani, Kalyani, Nadia, West Bengal 741235, India
Tel: +91-987-454-8900
E-mail: asmita.samadder@gmail.com

Background: Diabetic nephropathy (DN) is one of the major complications of chronic hyperglycaemia affecting normal kidney functioning. The ayurvedic medicine curcumin (CUR) is pharmaceutically accepted for its vast biological effects.
Objectives: The *Curcuma*-derived diferuloylmethane compound CUR, loaded on Poly (lactide-co-glycolic) acid (PLGA) nanoparticles was utilized to combat DN-induced renal apoptosis by selectively targeting and modulating Bcl2.
Methods: Upon *in silico* molecular docking and screening study CUR was selected as the core phytocompound for nanoparticle formulation. PLGA-nano-encapsulated-curcumin (NCUR) were synthesized following standard solvent displacement method. The NCUR were characterized for shape, size and other physico-chemical properties by Atomic Force Microscopy (AFM), Dynamic Light Scattering (DLS) and Fourier-Transform Infrared (FTIR) Spectroscopy studies. For *in vivo* validation of nephro-protective effects, *Mus musculus* were pre-treated with CUR at a dose of 50 mg/kg b.w. and NCUR at a dose of 25 mg/kg b.w. (dose 1), 12.5 mg/kg b.w (dose 2) followed by alloxan administration (100 mg/kg b.w) and serum glucose levels, histopathology and immunofluorescence study were conducted.
Results: The *in silico* study revealed a strong affinity of CUR towards Bcl2 (dock score −10.94 Kcal/mol). The synthesized NCUR were of even shape, devoid of cracks and holes with mean size of ~80 nm having −7.53 mV zeta potential. Dose 1 efficiently improved serum glucose levels, tissue-specific expression of Bcl2 and reduced glomerular space and glomerular sclerosis in comparison to hyperglycaemic group.
Conclusion: This study essentially validates the potential of NCUR to inhibit DN by reducing blood glucose level and mitigating glomerular apoptosis by selectively promoting Bcl2 protein expression in kidney tissue.

Keywords: PLGA encapsulated nano-curcumin, in silico molecular docking, Bcl2, glomerulus, kidney, nanomedicine

INTRODUCTION

Diabetes Mellitus (DM) can be defined as chronic hyperglycemia [1] and is associated with glucose intolerance where fasting blood glucose level remains greater than 100 mg/dL and post-prandial blood glucose is greater than 200 mg/dL [2]. DM can be categorized into two types: type 1 diabetes mellitus (T1DM) and type 2 diabetes mellitus (T2DM) [3]. T1DM is

classified in terms of autoimmune destruction of pancreatic β cells and essentially characterized by the absence of ketosis. Insulin resistance plays a vital role in T2DM, where persistent high blood glucose, impaired glucose tolerance, and modulated peripheral glucose uptake can lead to several problems involving microvascular and macrovascular complications. Microvascular complications include nephropathy, neuropathy, and retinopathy, and macrovascular complications include stroke and myocardial infarction [4]. Hyperglycemia is strongly correlated with chronic renal diseases. Persistently elevated blood glucose increases organ-specific oxidative stress and is accompanied by low- or high-grade systemic inflammation, triggering inflammation mediators like interleukin-6 (IL-6) and tumor necrosis factor-a (TNF-α). In the context of kidney diseases, this causes pertinent damage to the glomerular architecture and robustness, causing malfunctioning of the kidney. Damage is imparted to the endothelial cells of the glomerulus, smooth muscle cells, mesangial cells, podocytes, tubular epithelial cells, and collecting duct cells [5]. These cells together modulate various kidney-related parameters like urea and creatinine, often progressing toward end-stage renal disease (ESRD) [5]. This pathophysiological state is often termed diabetic nephropathy (DN), which is clinically characterized by a gradual increase in albuminuria and a resultant decline in the glomerular filtration rate (GFR). Excessive deposition of extracellular matrix (ECM) proteins like fibronectin and collagen IV leads to the thickening of the glomerular basement membrane (GBM), enlargement of glomerular capillaries, mesangial expansion, and renal hypertrophy, which are diagnostic parameters of the disease in preclinical models [6, 7]. Thus, in the context of DN, therapeutic management targets effective controlling of oxidative stress, nitrosative stress, the polyol pathway (involving the Renin-Angiotensin-Aldosterone system), inflammasomes, ECM modifications, and fibrosis [8].

In silico techniques allow the virtual screening of thousands of compounds in a feasible time frame, saving initial expenses and animals for the hit selection and enhancing the probability of recognizing the necessary therapeutic candidates [9] and their accompanying signaling cascades. This computer-based study analyzed the configuration and alignment of ligands into the active sites of biomolecular protein targets [10, 11]. Thus, molecular docking determines the active binding residues that bind with the ligand to generate the most computationally stable shape of the ligand-receptor complex to minimize the energy of interactions between the ligand and the receptor [12]. This aids in tracing the signaling cascades on which the drug operates to produce a biological response, which, if validated by experimental investigations, can help in understanding the targets of newly discovered drug molecules [13, 14].

Phytocompounds provide us with a vast repertoire of chemical compounds that are novel in terms of structure-function relationships and have the potential to form putative clinically relevant drug candidates [15]. Plants in the genus *Curcuma* are known to have a vast range of pharmaco-active compounds, of which the principal compound curcumin (CUR) ([1E,6E]-1,7-bis [4-hydroxy- 3-methoxyphenyl] -1,6- heptadiene-3,5-dione) has been extensively studied for its anti-proliferative, anti-cancer, anti-inflammatory, anti-apoptotic, anti-diabetic, and anti-fibrotic properties [16]. CUR was chosen for this study due to a number of biological qualities, including its ability to scavenge cellular reactive oxygen species, reduce inflammation, render natural restoration of stress-induced tissue damage, and fight against cancer generation [17]. However, CUR therapy comes with the drawback of poor bio-availability and low plasma and tissue-specific concentrations due to rapid metabolization and poor dietary absorption [18]. To overcome this problem, nanoparticles were strategically formulated, and due to their smaller size, negative zeta potential, and improved sustained and burst release capabilities they have better bio-distribution, bioavailability, cell and tissue absorption, penetration, and uptake [19]. Therefore, the main objectives of this study were to: (i) formulate biodegradable poly lactic-co-glycolic acid (PLGA) polymer-based nano particles using CUR as the drug component, (ii) determine the physicochemical characterizations and encapsulation efficacy of the CUR nano-particles (NCURs) before administration in the mice model, (iii) predict the target protein of CUR (the core phyto-compound of the NCURs) and verify its interaction with anti-apoptotic protein B-cell lymphoma 2 (Bcl2) via *in silico* molecular docking study, and (iv) validate the role of the NCURs to modulate the target protein Bcl2 to mitigate apoptosis of glomerular cells and improve diabetes-induced nephropathy in the experimental diabetic mice model.

MATERIALS AND METHODS

1. Chemicals and reagents

All the chemicals and reagents used in this study were of analytical grade and purchased from Sigma Aldrich, USA, and Merck, Germany unless mentioned otherwise.

 https://doi.org/10.3831/KPI.2024.27.1.1

2. *In silico* docking study for predicting the active binding and targeting of CUR with the anti-apoptotic protein Bcl2

CUR was the phyto-compound of focus in this study. The two-dimensional (2D) chemical structure of CUR was obtained from PubChem and designed in ChemDraw Ultra 8.0 software, which was then modified to its three-dimensional (3D) model using Chem3D Ultra 8.0, followed by energy minimization to get the optimum configuration. The Protein Data Bank (PDB) was chosen as the most suitable site for downloading the Bcl2 protein structure, and its PDB ID is 6GL8 [20]. For the docking study, the desired protein was constructed by withdrawing water molecules and adding hydrogen atoms. Arguslab 4.0.1. was used for the docking operations since it enables flexible docking. The co-crystallized molecule ~{N}-(4-hydroxyphenyl)-3-[6-[[(3~{S})-3-(morpholin-4-ylmethyl)-3,4-dihydro-1~{H}-.isoquinolin-2-yl]carbonyl]-1,3-benzodioxol-5-yl]-~{N}-phenyl-5,6,7,8-tetrahydroindolizine-1-carboxamide served as the template to determine the active pocket of the protein for interactions. After successful docking, the ligand-receptor complex conformation with the lowest binding energy was identified, and Discovery Studio was utilized to interpret the patterns of interaction to find the important amino acid residues and corresponding linkages binding the protein with the distinct groups of the ligand.

3. Preparation of the PLGA-encapsulated CUR nanoparticles (NCURs)

The NCURs were formulated using a standard solvent displacement method under optimal conditions [21]. In brief, 20 mg of CUR and 50 mg of PLGA were dissolved in 2 mL of acetone (organic solvent). The stabilizer mixture was prepared by dissolving 200 g of F68 (1% polyoxyethylene–polyoxypropylene) stabilizer in 20 mL of the aqueous solution, to which the organic mixture was added in a dropwise manner with continuous stirring using a magnetic stirrer at room temperature until the organic solvent completely evaporated. At the end of the reaction process, the final weight of the NCURs was 212 mg. The initial concentration of CUR used was 20 mg, and the final yield of NCURs weighed 212 mg, approximately ten times the initial drug quantity. Thus, a ten-fold increase in yield was observed after the formation of the NCURs [22]. Hence, 1 mg of NCURs contains a ten-fold reduction in the amount of CUR (i.e., 0.1 mg of CUR as the core component).

4. Characterization of the NCURs by atomic force microscopic (AFM) studies and dynamic light scattering (DLS)

Atomic Force Microscopic (AFM) imaging was conducted to determine the size, shape, and smoothness of the newly formed NCURs [23, 24]. AFM images were recorded in amplitude and tapping modes, which were observed and analyzed using WSxM 5.0 Develop 7.0 software. The Dynamic Light Scattering (DLS) study was conducted to determine the zeta potential of the NCURs using a Nano-ZS instrument (Malvern, UK), following standard practice [23, 24].

5. Assessment of the functional groups in the NCURs by fourier-transform infrared spectroscopic (FTIR) analysis

The Fourier-transform infrared spectroscopic (FTIR) spectra of CUR and the newly formed NCURs were obtained using a Perkin Elmer cFTIR Spectrometer, Model- Spectrum Two, Sl (No. 106422).

6. Animals

Healthy inbred 6-8 week Swiss albino mice (*Mus musculus*), weighing around 25 g, were housed in an environmentally controlled room (24-26 ± 2℃; humidity 55 ± 5%, 12-hour light/dark cycle) with standard food and water *ad libitum*. All experiments were conducted per the guidelines of the Institutional Animal Ethical Committee (IAEC) of the University of Kalyani, West Bengal, India (approval number 892/GO/Re/S/0l/CPCSEA).

7. Induction of diabetes

Diabetes was induced in the mice by a single intraperitoneal (i.p.) injection of Alloxan monohydrate (ALX) dissolved in sterile normal saline at a dose of 100 mg/kg body weight (b.w.). On the fifth day after diabetic induction, blood was collected to measure the blood glucose level [25, 26].

8. Dose selection for CUR and the NCURs

A range-finding trial was performed where CUR and NCURs were administrated orally, and the blood glucose levels were measured in each case [22]. The dose of 50 mg/kg b.w. for

CUR and 25 mg/kg b.w. and 12.5 mg/kg b.w. for NCURs were selected according to the results of the range-finding trial based on the reduction in the blood glucose level when exposed to ALX. The experiment consisted of six animals in each group, listed below.

Group 1: Control: untreated control.

Group 2: ALX: single i.p. dose of 100 mg/kg b.w.

Group 3: CUR + ALX: 50 mg/kg b.w. of CUR was fed orally for seven days + ALX.

Group 4: NCUR-1 + ALX: 25 mg/kg b.w. of the NCURs was fed orally for seven days + ALX.

Group 5: NCUR-2 + ALX: 12.5 mg/kg b.w. of the NCURs was fed orally for seven days + ALX.

9. Measurement of serum glucose

Blood glucose was measured at the end of the treatment period using a standard GOD-POD Glucose kit (Autospan) from Cogent Diagnostics Ltd., India [14].

10. Biochemical assay

A kit-based assay for urea, creatinine, aspartate aminotransferase (AST), and alanine aminotransferase (ALT) was performed as per the standard practice [27].

11. Histopathological study of kidney tissues

Kidney tissues were fixed in 10% neutral buffered formalin followed by a standard dehydration method and paraffin embedding [28]. The histopathological slides were stained using Haematoxylin-Eosin (H&E), and the changes were observed using a Labomed Lx300 microscope at 10× objective, and vital observations were noted.

12. Assessment of the Bcl2 protein expression level by immunofluorescence

The Bcl2 protein expression level in kidney tissue from the control and experimental mice groups were detected following the standard practice of immunofluorescence using an anti-Bcl2 primary antibody (Santa Cruz Biotechnology, Inc., USA), FITC (Fluorescein-5-isothiocyanate) conjugated secondary antibody (Sigma, USA), and counterstained using DAPI (4′,6-diamidino-2-phenylindole). The images were photographed using an inverted fluorescence microscope (Carl Zeiss Axio Vert A1-FL-LED) at 10× magnification. The intensity of fluorescence was also measured using Image J software under a specific plugin size [23].

13. Statistical analysis

Data were analyzed using a student's t-test and one-way ANOVA after executing three independent experiments. The means and Standard Error were calculated as necessary.

RESULTS

1. Analysis of the *in silico* docking study of CUR targeting the anti-apoptotic protein Bcl2

Molecular docking is a computational tool that helps in understanding the binding affinity of ligand and protein complexes through their amino acid interactions. Molecular docking studies of Bcl2 (protein) and CUR (ligand) revealed a binding score of –10.94 Kcal/mol. The hydroxyl groups of both 2-methoxyphenol interact with ARG146, GLU136, and ASP111, and the carbonyl moieties interact with MET115 and PHE153 through hydrogen bonding, resulting in the stability of the drug-protein complex. Further, both 2-methoxyphenol moieties of the ligand were dominated by hydrophobic interactions with the residues LEU137, PHE104, and PHE112. Therefore, according to the docking experiment, the ligand is retained in the protein cavity via hydrogen bonds and hydrophobic interactions (Fig. 1).

2. Assessment of the size and zeta potential of the NCURs

AFM helps demonstrate the surface topology, shape, and size of any particle, while DLS measures the zeta potential of the nanoparticles. The AFM and DLS data revealed that the NCURs had a mean diameter of 80 nm, were spherical with smooth surfaces, and had no cracks or holes (Fig. 2A-C). The nanoparticles had a zeta potential of -7.53 mV. The Fast Fourier Transform (FFT) image of the topographic planer signal revealed a uniform spatial frequency (Fig. 2D).

 https://doi.org/10.3831/KPI.2024.27.1.1

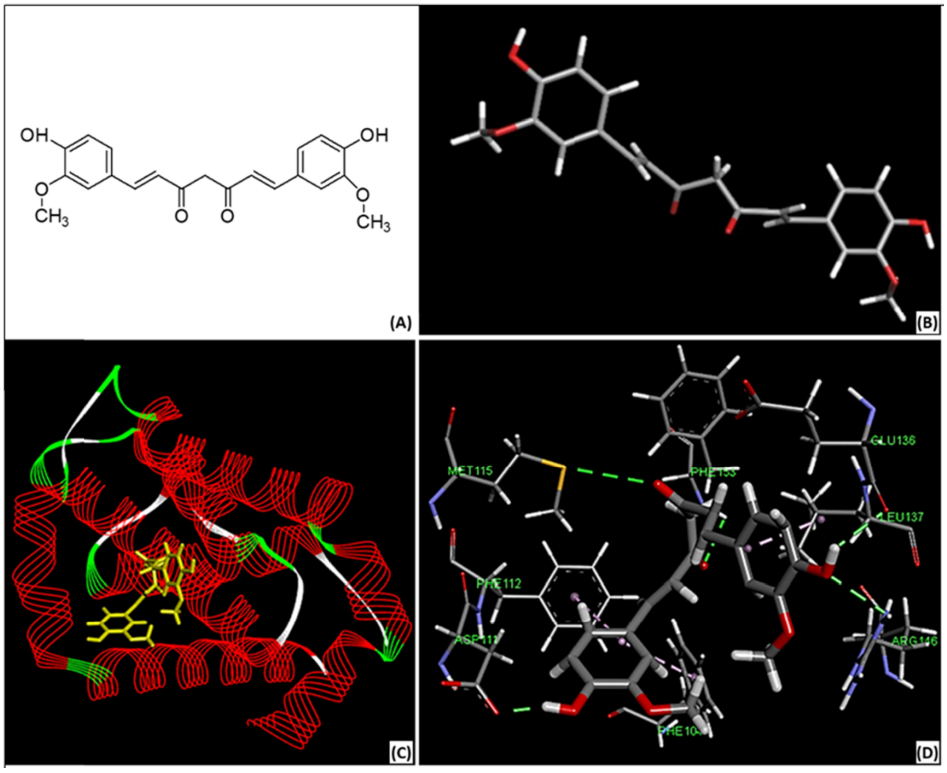

Figure 1. (A) 2D structure of CUR with atom symbols, (B) 3D structure of CUR, (C) molecular docking study of CUR and Bcl2 showing the protein-ligand binding pose, (D) the best docked confirmation of protein-ligand complex.

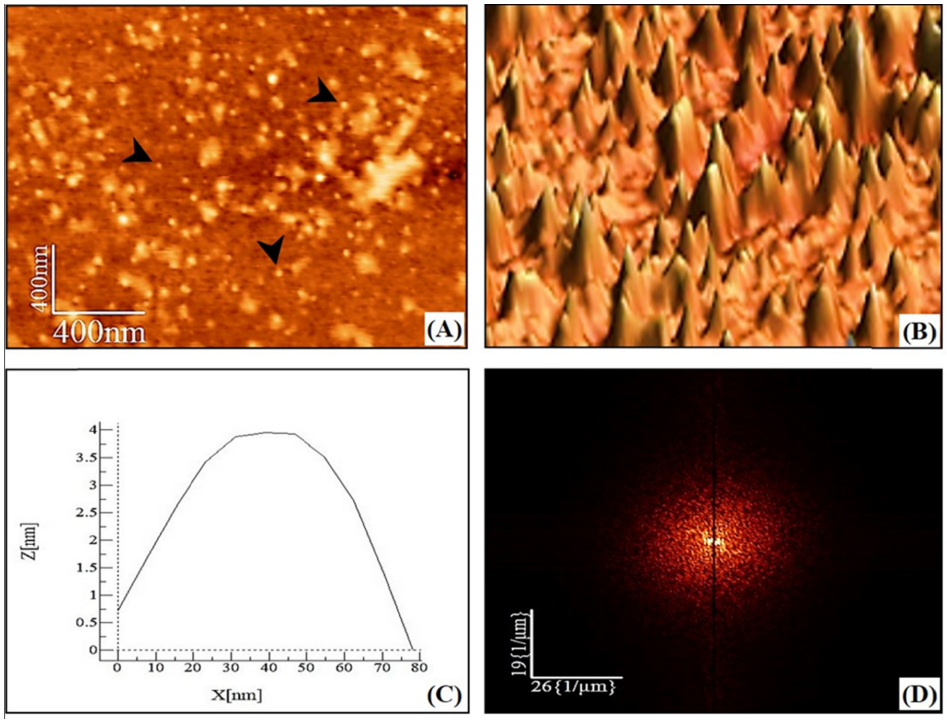

Figure 2. AFM study of NCUR: (A, B) 2D and 3D view of NCUR (arrow-head indicates a single nanoparticle), (C) size profile of NCUR, (D) FFT analysis.

3. FTIR analysis for the functional groups of CUR and the NCURs

FTIR Spectroscopy utilizes infrared light to scan a particular compound and provide the functional groups as spectral peaks. The FTIR spectra of CUR and the NCURs showed a wide peak at 3,200-3,600 cm^{-1} and a sharp band at 3,429.6 cm^{-1} due to the presence of -OH groups. The strong peak at 2,923.93 cm^{-1} in

CUR and 2,921.65 cm^{-1} in the NCURs appears due to asymmetric CH stretching of either CH_3 or OCH_3 groups. The intense band observed at 1,758.3 cm^{-1} for the NCURs is attributed to the stretching vibration of the carbonyl groups present in the two monomers of PLGA. The CUR spectrum exhibited a sharp peak at 1,508.6 cm^{-1}, which was attributed to the ν(C = O) peak for CUR. The sharp peaks at 1633.04 cm^{-1} in the NCURs and 1,628.12 cm^{-1} in CUR are attributed to the C = O

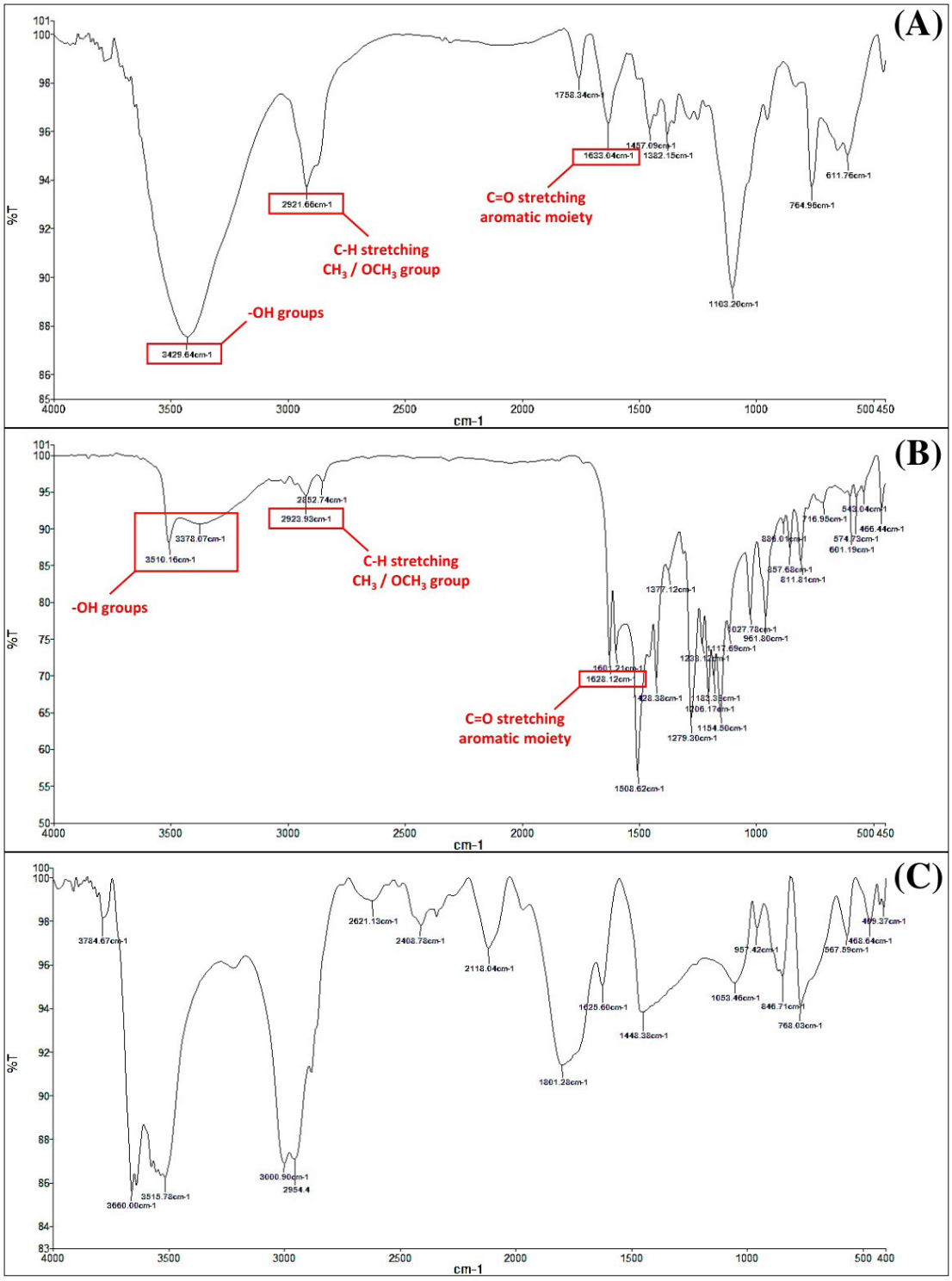

Figure 3. (A) FTIR study of NCUR, (B) FTIR study of CUR, (C) FTIR study of blank PLGA.

 https://doi.org/10.3831/KPI.2024.27.1.1

stretching of the aromatic moiety of curcumin. In addition to the C-H stretching, bending vibrations of the C-H group were observed at 1,279.3 cm^{-1}. A sharp peak at 1,103.2 cm^{-1} was observed, which was ascribed to the C-O stretching of the ester group present in the NCURs. Similar appearances of the functional groups of CUR and NCUR confirm the presence of CUR inside the PLGA nanoparticles. The IR spectra of PLGA reflect the presence of carbonyl, alcoholic OH, and ester C-O groups. The sharp peak at 1,801.2 cm^{-1} is attributed to the presence of carbonyl C = O stretching vibrations. The band near 3,500 cm^{-1} appears due to the stretching of the end O-H group of the gly-

Table 1. Serum blood glucose levels of control and experimental set

Group	Serum glucose level (mg/dL)
Control	124.04 ± 1.33
ALX	195.46 ± 1.27##
CUR + ALX	116 ± 2.19**
NCUR-1 + ALX	128 ± 1.8**
NCUR-2 + ALX	126 ± 2.01**

Data shows actual differences between control and ALX and that of CUR, NCUR-1 + ALX and NCUR-2 + ALX.
##p < 0.01 *vs* Control; **p < 0.01 *vs*. ALX treated group were considered significant.

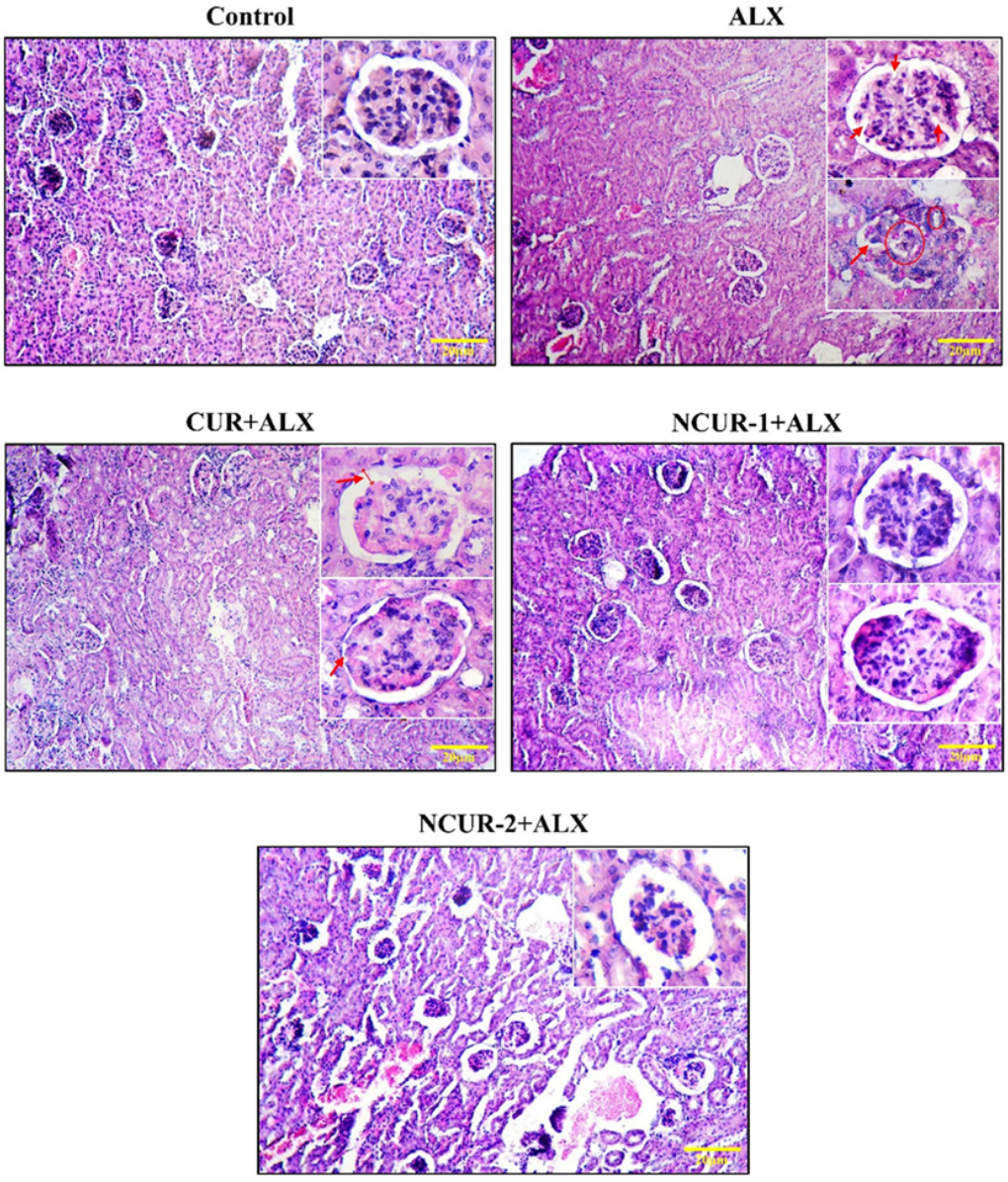

Figure 4. Histological sections of kidney in control and experimental mice group.

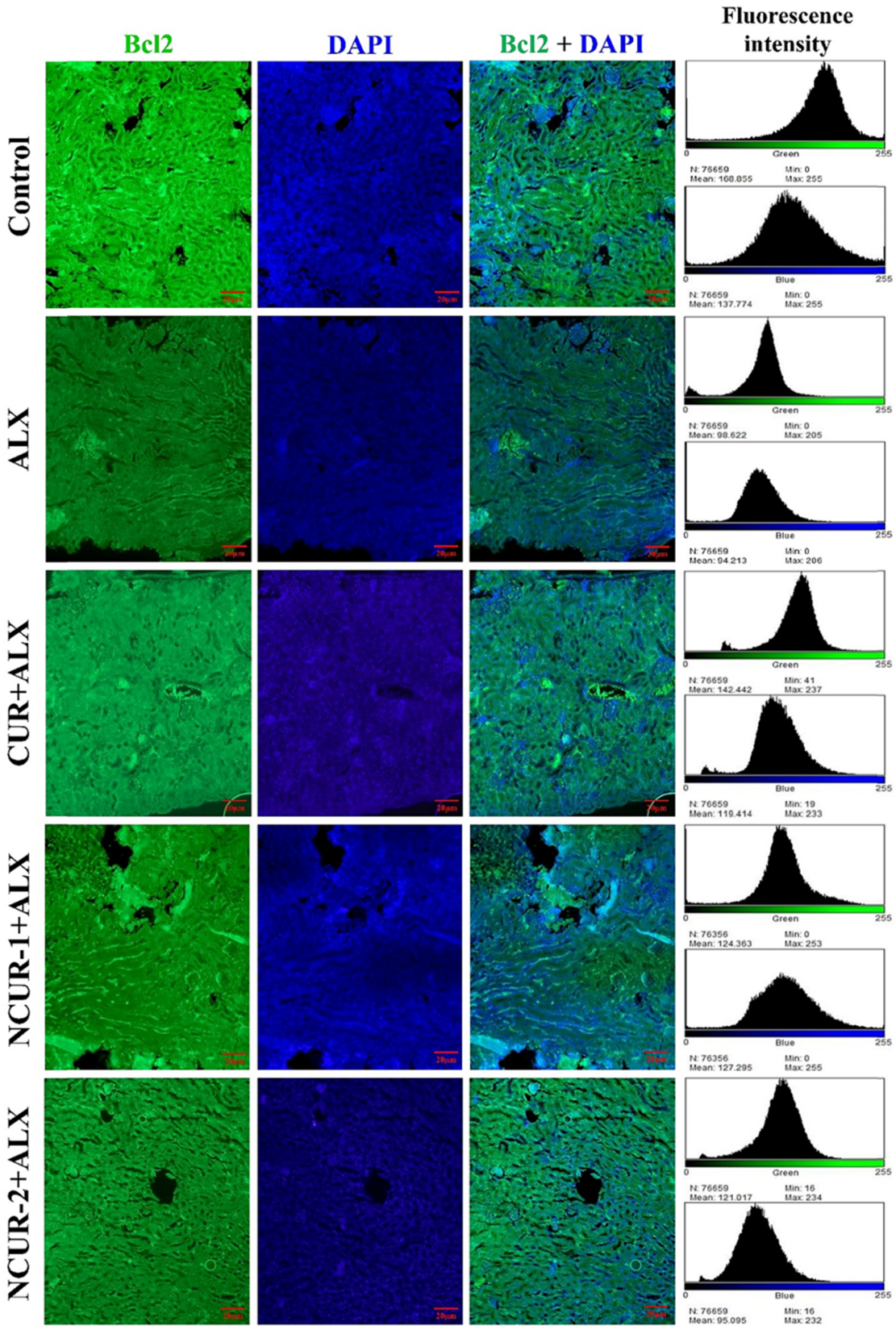

Figure 5. Immunofluorescence study of Bcl2 protein counter stained with DAPI, along with the fluorescence intensity study (scale bar 20 μm).

 https://doi.org/10.3831/KPI.2024.27.1.1

colic acid part. The peak appearing at 1,053.4 cm^{-1} is ascribed to the C-O stretching of the ester fragment. These peaks suggest the presence of ester linkage in addition to the functional groups and different bonds of lactic acid and glycolic acid in the PLGA polymer (Fig. 3).

4. Assessment of blood glucose levels

Monitoring the blood glucose level is an important parameter for understanding the homeostatic state of glucose in the body and is severely upregulated in diabetes. The blood glucose data revealed that the CUR + ALX, NCUR-1 + ALX, and NCUR-2 + ALX groups inhibited the ALX-induced increase in fasting serum glucose levels in mice (Table 1). It may be noted that the NCURs had a better inhibition of this increase due to the ten-fold reduction in drug content in the PLGA nanocapsule.

5. Histopathological findings in kidney tissues

Histopathology helps demonstrate the structural changes of tissue organization in pathological samples. The Alloxan group showed a reduction in the glomerular space along with sclerotic lesions. The CUR pre-treatment reduced the sclerotic lesions after ALX administration but failed to restore appropriate glomerular space completely (arrow and circular marks indicate sclerotic lesions). However, the NCUR-1 + ALX group showed the best results where the glomerular space was restored, and the kidney tissue displayed no sclerotic lesions, nearly similar to the control group. The NCUR-2 + ALX mice showed evenly spaced glomerular space and no sclerotic lesions, but better results were seen in the NCUR-1 + ALX group (Fig. 4).

6. Expression level of Bcl2 protein measured by immunofluorescence

Immunofluorescence can detect the relative expression and localization of target proteins in different experimental groups. The immunofluorescence results revealed that the CUR + ALX group and both the NCUR (NCUR-1 + ALX and NCUR-2 + ALX) groups showed a greater potential to modulate the anti-apoptotic protein Bcl2, thereby altering the effects of ALX. The NCURs had a better result based on the fact that the actual drug component present in the nano-core is ten-fold lower than in CUR (Fig. 5).

7. Assessment of the biochemical tests

The optimum levels of the metabolic nitrogen end products, urea and creatinine, indicate properly functioning kidneys, and

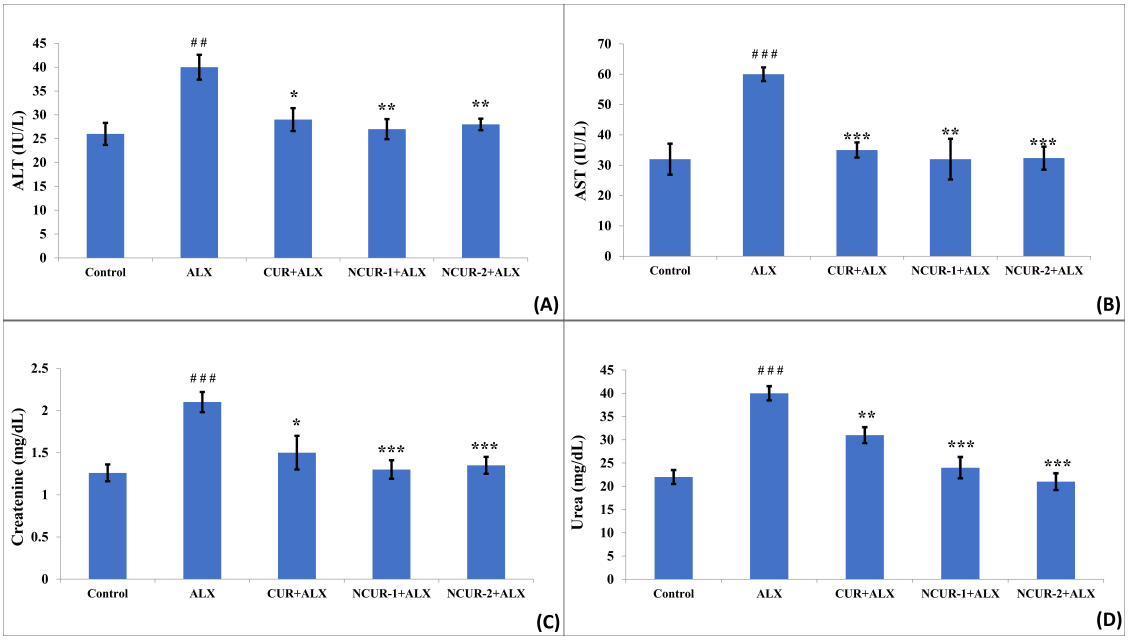

Figure 6. Graphical representation of liver and kidney function tests; (A) ALT, (B) AST, (C) Creatinine, (D) Urea. $^{\#\#}p < 0.01$ vs. Control, $^{\#\#\#}p < 0.001$ vs. Control; $^{*}p < 0.05$ vs. ALX, $^{**}p < 0.01$ vs. ALX, $^{***}p < 0.001$ vs. ALX.

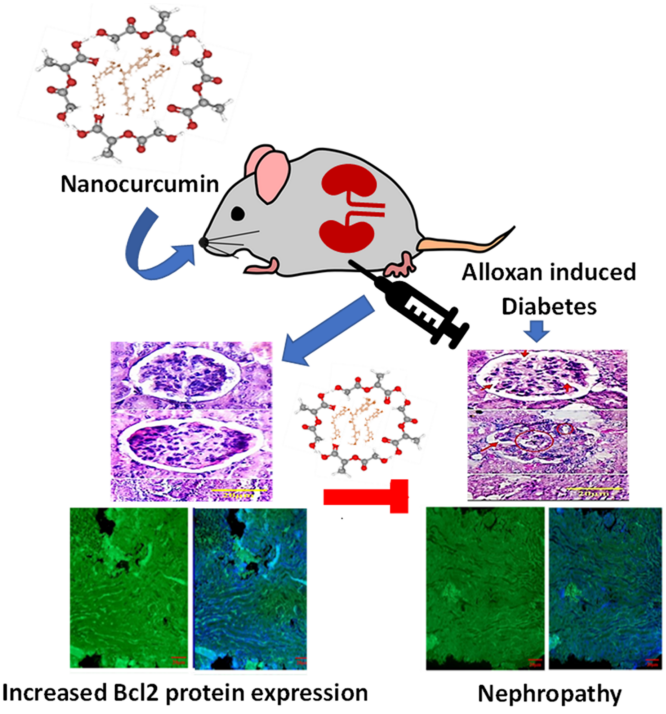

Figure 7. Overall representation of the role of NCUR to combat ALX induced DN.

aspartate aminotransferase (AST) and alanine transaminase (ALT) levels are indicative of a functional liver. The ALX treatment elevated all four of the parameters, and this increase was significantly inhibited by the CUR and NCUR treatments, with the best result seen in the NCUR doses, which were similar to the control group (Fig. 6).

DISCUSSION

This current study assessed the added advantage of NCURs over CUR pre-treatment in a diabetic-induced nephropathic mice model, thereby exploring the additional advantage of utilizing PLGA-encapsulated phytocompounds as a means of delivering drugs to enhance the therapeutic potential to prevent patho-physiological damage (Fig. 7). Oxidative stress, inflammation, altered kidney architecture, unstable blood glucose levels, creatinine, urea, AST, and ALT are among the key variables in the development of DN. This study implies that due to the side effects of several medicines used to treat DN, the phytocompound CUR and NCURs might contribute to improving the pathological alterations by inhibiting the extent of the initiation and progression of DN, with the NCURs showing the greatest efficiency.

DN is significantly characterized by the appearance of vascular and glomerular lesions and reduced GFR in diabetic patients. This is evidence that prolonged diabetes can affect kidney function [29, 30], and eventually can cause chronic kidney disease and ESRD [31]. DN affects several mediators that have direct roles in biological responses like cell proliferation, apoptosis, and ECM depositions [32]. Although the exact pathway that is followed in triggering apoptosis due to high blood glucose levels is not known, there is evidence from reports that high glucose concentrations promote apoptosis in the kidneys by targeting various cell types involving proximal and distal tubular epithelial cells [33-35]. Thus, the characteristic tubular apoptosis in the renal tubular cells plays an important role in explaining the characteristic histologic changes in the renal tubules of diabetic patients and thus links renal tubule atrophy with the progression of diabetes-induced nephropathy.

In silico structure-based molecular docking simulation studies help understand interaction modalities, predicting the affinity and specificity of ligands like phytocompounds towards their molecular targets. This *in silico* ligand docking study revealed effective interaction and good binding affinity of the drug towards its target, Bcl2, predicting the anti-apoptotic nature of CUR, which might help identify the signaling cascades involved in restricting the progression of DN.

Advances in nanotechnology have mediated drug development and allowed for the pharmaco-modulation of putative components providing the ability to fine-tailor drug candidates and improve their efficacy. For example, the Food and Drug Administration (U.S.A) has approved nontoxic and biodegradable PLGA as a biopolymer. PLGA-encapsulated nanoparticles have better bioavailability due to their nanoscale size, which enables nano-drugs to readily penetrate and overcome biological barriers, facilitating simple internalization. Nano-drugs have been shown to have better results than their non-nano counterparts in controlling or inhibiting DN complications. However, CUR and NCUR pre-treatments restricted changes in the blood glucose levels, pointing to the potential of CUR in optimizing diabetes-induced glucose imbalance. However, since there is a ten-fold reduction in the amount of the drug that gets incorporated in the PLGA capsule during the formulation process, the actual drug content in the PLGA capsules is ten times less than that of CUR. Thus, the results with CUR and NCUR, even if showing similar results, delineate the fact that each 1 mg of NCURs holds 0.1 mg of CUR, while each 1 mg of CUR is 1 mg of curcumin, thereby signifying that the NCURs are more effec-

 https://doi.org/10.3831/KPI.2024.27.1.1

tive than CUR.

Apoptosis, a form of programmed cell death that occurs normally during organ development as well as aging, maintains the homeostasis of cell populations in tissues. There are various stimuli that trigger apoptosis, and apoptosis is characterized by membrane blebbing, cell shrinkage, deoxyribonucleic acid (DNA) fragmentation, and nuclear condensation. The anti-apoptotic protein Bcl2 plays a major role in cell survival by inhibiting the release of cytochrome C from the mitochondria and other downstream proteases and the subsequent activation of the initiator caspase 9. In this study, the expression of Bcl2 was the highest in the kidney tissue sections of the NCUR mice group, verifying the histo-pathological findings of the kidney tissue. Thus, docking studies portraying the Bcl2 and CUR interaction offer atomic-level detail on the complex formation between the ligand and the target protein, which is essential in predicting the possible pathways for therapeutic strategies to improve the lives of patients with diabetes suffering from nephropathic complications.

CONCLUSION

Therefore, this present study pinpoints the added advantage of *in silico* molecular docking-based predictions of target drug-protein interactions and the efficacious role of nano-based drug formulation. These two technical advancements of integrative therapy will help in rerouting therapeutic strategies for "bio-target" based drug development and "target-specific" drug delivery in the near future to treat a number of disorders in a cost-effective manner.

ABBRIBIATIONS

AFM, Atomic Force Microscopy; ALT, Alanine aminotransferase; ALX, Alloxan monohydrate; ANOVA, Analysis of Variance; AST, Aspartate aminotransferase; b.w., Body weight; Bcl2, B-cell lymphoma 2 protein; CPCSEA, Committee for the Purpose of Control and Supervision of Experiments on Animals; CUR, Curcumin; DAPI, 4′,6-diamidino-2-phenylindole; DLS, Dynamic Light Scattering; DN, Diabetic Nephropathy; DNA, Deoxyribonucleic Acid; ECM, Extracellular Matrix; ESRD, End-Stage Renal Disease; FFT, Fast Fourier Transform; FITC, Fluorescein-5-isothiocyanate; FTIR, Fourier-Transform Infrared Spectroscopy; GBM, Glomerular Basement Membrane; GFR, Glomerular Filtration Rate; GOD-POD, Glucose oxidase - peroxidase; H&E, Haematoxylin-Eosin staining; i.p., intraperitoneal; IAEC, Institutional Animal Ethical Committee; IL-6, Interleukin-6; mV, Millivolts; NCUR, PLGA-nano-encapsulated-curcumin; nm, Nanometres; PDB, Protein Data Bank; PLGA, Poly (lactide-co-glycolic) acid; T1DM, Type 1 diabetes mellitus; T2DM, Type 2 diabetes mellitus; TNF-α, Tumour Necrosis Fator-α.

ACKNOWLEDGEMENTS

The authors acknowledge the Department of Zoology and S.N. Bose Innovation Centre, University of Kalyani and GIPER, Uttarakhand for providing the infrastructural and instrumentation support for this study. SD, PS and RD extend their thankfulness to UGC for the SRF-fellowship. AC is grateful to University of Kalyani for URS (University Research Scholar) fellowship. BB is grateful to Govt. of West Bengal for SVMCM fellowship.

CONFLICTS OF INTEREST

The authors declare no conflicts of interest in this work.

FUNDING

This research has been funded by SERB (DST) (Grant No. ECR/2017/000355/LS) and UGC, New Delhi for the UGC-BSR (Grant no: F.30-488/2019 [BSR]) sanctioned to Dr. Asmita Samadder. The authors would also like to acknowledge the University of Kalyani for providing Personal Research Grant which were partly used for the research.

ORCID

Asmita Samadder, https://orcid.org/0000-0002-3604-7404
Banani Bhattacharjee, https://orcid.org/0000-0001-6290-3430
Sudatta Dey, https://orcid.org/0000-0003-4867-1674
Arnob Chakrovorty, https://orcid.org/0000-0003-4147-4651
Rishita Dey, https://orcid.org/0000-0002-6584-8083
Priyanka Sow, https://orcid.org/0000-0002-0280-1077
Debojyoti Tarafdar, https://orcid.org/0000-0001-8358-9196
Maharaj Biswas, https://orcid.org/0000-0001-5142-3730
Sisir Nandi, https://orcid.org/0000-0002-9960-6584

REFERENCES

1. Kaul K, Tarr JM, Ahmad SI, Kohner EM, Chibber R. Introduction to diabetes mellitus. In: Ahmad SI, editor. Diabetes: an old disease, a new insight. New York: Springer; 2013. p. 1-11.
2. Guerrero-Romero F, Violante R, Rodríguez-Morán M. Distribution of fasting plasma glucose and prevalence of impaired fasting glucose, impaired glucose tolerance and type 2 diabetes in the Mexican paediatric population. Paediatr Perinat Epidemiol. 2009;23(4):363-9.
3. Forouhi NG, Wareham NJ. Epidemiology of diabetes. Medicine. 2014;42(12):698-702.
4. Ohiagu FO, Chikezie PC, Chikezie CM. Pathophysiology of diabetes mellitus complications: metabolic events and control. Biomed Res Ther. 2021;8(3):4243-57.
5. Jha JC, Banal C, Chow BS, Cooper ME, Jandeleit-Dahm K. Diabetes and kidney disease: role of oxidative stress. Antioxid Redox Signal. 2016;25(12):657-84.
6. Ni WJ, Tang LQ, Wei W. Research progress in signalling pathway in diabetic nephropathy. Diabetes Metab Res Rev. 2015;31(3): 221-33.
7. Kanwar YS, Wada J, Sun L, Xie P, Wallner EI, Chen S, et al. Diabetic nephropathy: mechanisms of renal disease progression. Exp Biol Med. 2008;233(1):4-11.
8. Wang S, Zhao X, Yang S, Chen B, Shi J. Salidroside alleviates high glucose-induced oxidative stress and extracellular matrix accumulation in rat glomerular mesangial cells by the TXNIP-NLRP3 inflammasome pathway. Chem Biol Interact. 2017; 278:48-53.
9. Liu Z, Liu Y, Zeng G, Shao B, Chen M, Li Z, et al. Application of molecular docking for the degradation of organic pollutants in the environmental remediation: a review. Chemosphere. 2018; 203:139-50.
10. Torres PHM, Sodero ACR, Jofily P, Silva-Jr FP. Key Topics in Molecular Docking for Drug Design. Int J Mol Sci. 2019;20(18): 4574.
11. Kitchen DB, Decornez H, Furr JR, Bajorath J. Docking and scoring in virtual screening for drug discovery: methods and applications. Nat Rev Drug Discov. 2004;3(11):935-49.
12. Nandi S, Bagchi MC. 3D-QSAR and molecular docking studies of 4-anilinoquinazoline derivatives: a rational approach to anticancer drug design. Mol Divers. 2010;14(1):27-38.
13. Sow P, Dey S, Dey R, Majumder A, Nandi S, Bera M, et al. Poly lactide-co-glycolide encapsulated nano-curcumin promoting antagonistic interactions between HSP 90 and XRCC1 proteins to prevent cypermethrin-induced toxicity: an in silico predicted in vitro and in vivo approach. Colloids Surf B Biointerfaces. 2022;220:112905.
14. Dey R, Nandi S, Samadder A. "Pelargonidin mediated selective activation of p53 and parp proteins in preventing food additive induced genotoxicity: an in vivo coupled in silico molecular docking study". Eur J Pharm Sci. 2021;156:105586.
15. Dey S, Nagpal I, Sow P, Dey R, Chakrovorty A, Bhattacharjee B, et al. Morroniside interaction with poly (ADP-ribose) polymerase accentuates metabolic mitigation of alloxan-induced genotoxicity and hyperglycaemia: a molecular docking based *in vitro* and *in vivo* experimental therapeutic insight. J Biomol Struct Dyn. 2023:1-18.
16. Hewlings SJ, Kalman DS. Curcumin: a review of its effects on human health. Foods. 2017;6(10):92.
17. Giordano A, Tommonaro G. Curcumin and cancer. Nutrients. 2019;11(10):2376.
18. Anand P, Kunnumakkara AB, Newman RA, Aggarwal BB. Bioavailability of curcumin: problems and promises. Mol Pharm. 2007;4(6):807-18.
19. Das S, Das J, Samadder A, Paul A, Khuda-Bukhsh AR. Strategic formulation of apigenin-loaded PLGA nanoparticles for intracellular trafficking, DNA targeting and improved therapeutic effects in skin melanoma in vitro. Toxicol Lett. 2013;223(2):124-38.
20. Casara P, Davidson J, Claperon A, Le Toumelin-Braizat G, Vogler M, Bruno A, et al. S55746 is a novel orally active BCL-2 selective and potent inhibitor that impairs hematological tumor growth. Oncotarget. 2018;9(28):20075-88.
21. Fessi H, Puisieux F, Devissaguet JP, Ammoury N, Benita S. Nanocapsule formation by interfacial polymer deposition following solvent displacement. Int J Pharm. 1989;55(1):R1-4.
22. Samadder A, Abraham SK, Khuda-Bukhsh AR. Nanopharmaceutical approach using pelargonidin towards enhancement of efficacy for prevention of alloxan-induced DNA damage in L6 cells via activation of PARP and p53. Environ Toxicol Pharmacol. 2016;43:27-37.
23. Samadder A, Das J, Das S, De A, Saha SK, Bhattacharyya SS, et al. Poly(lactic-co-glycolic) acid loaded nano-insulin has greater potentials of combating arsenic induced hyperglycemia in mice: some novel findings. Toxicol Appl Pharmacol. 2013;267(1):57-73.
24. Samadder A, Das S, Das J, Khuda-Bukhsh AR. Relative efficacies of insulin and poly (lactic-co-glycolic) acid encapsulated nano-insulin in modulating certain significant biomarkers in arsenic intoxicated L6 cells. Colloids Surf B Biointerfaces. 2013;109:10-9.
25. Samadder A, Dey S, Sow P, Das R, Nandi S, Das J, et al. Phytochlorophyllin prevents food additive induced genotoxicity and mitochondrial dysfunction via cytochrome c mediated pathway in mice model. Comb Chem High Throughput Screen. 2021;

24(10):1618-27.
26. Samadder A, Chakraborty D, De A, Bhattacharyya SS, Bhadra K, Khuda-Bukhsh AR. Possible signaling cascades involved in attenuation of alloxan-induced oxidative stress and hyperglycemia in mice by ethanolic extract of syzygium jambolanum: drug-DNA interaction with calf thymus DNA as target. Eur J Pharm Sci. 2011;44(3):207-17.
27. Moss DW, Henderson AR. Clinical enzymology. In: Burtis CA, Ashwood ER, Tietz NW, editors. Tietz textbook of clinical chemistry. 3rd ed. Philadelphia: W.B Saunders Company; 1999. p. 617-721.
28. Fischer AH, Jacobson KA, Rose J, Zeller R. Hematoxylin and eosin staining of tissue and cell sections. CSH Protoc. 2008;2008: pdb.prot4986.
29. Weil EJ, Lemley KV, Mason CC, Yee B, Jones LI, Blouch K, et al. Podocyte detachment and reduced glomerular capillary endothelial fenestration promote kidney disease in type 2 diabetic nephropathy. Kidney Int. 2012;82(9):1010-7.
30. Barnes DJ, Pinto JR, Davison AM, Cameron JS, Grunfeld JP, Kerr DNS, et al. The patient with diabetes mellitus. In: Davison AM, editor. Oxford textbook of clinical nephrology. 2nd ed. Oxford: Oxford University Press; 1998.
31. Lim AKh. Diabetic nephropathy - complications and treatment. Int J Nephrol Renovasc Dis. 2014;7:361-81.
32. Martindale JL, Holbrook NJ. Cellular response to oxidative stress: signaling for suicide and survival. J Cell Physiol. 2002; 192(1):1-15.
33. Allen DA, Harwood S, Varagunam M, Raftery MJ, Yaqoob MM. High glucose-induced oxidative stress causes apoptosis in proximal tubular epithelial cells and is mediated by multiple caspases. FASEB J. 2003;17(8):908-10.
34. Verzola D, Bertolotto MB, Villaggio B, Ottonello L, Dallegri F, Salvatore F, et al. Oxidative stress mediates apoptotic changes induced by hyperglycemia in human tubular kidney cells. J Am Soc Nephrol. 2004;15 Suppl 1:S85-7.
35. Dey S, Dey R, Sow P, Bhattacharjee B, Chakrovorty A, Samadder A, et al. An in silico validated study of nano-curcumin in attenuation of food-additive induced diabetic state and genotoxicity by selective modulation of DNA damage response proteins in mice model: a multi-parametric approach. In: Das M, editor. Book of abstracts. Vol. 6, (Agriculture, fisheries and animal science, botany, physiology, zoology) of the fifth regional science and technology congress, region three. Kolkata: West Bengal State University; 2023. p. 112-3.